Unrepeated 200-km transmission of 40-Gbit/s 16-QAM signals using digital coherent receiver

Yojiro Mori*, Chao Zhang, Koji Igarashi, Kazuhiro Katoh, and Kazuro Kikuchi

Department of Electronic Engineering,
The University of Tokyo,
7-3-1 Hongo, Bunkyo-ku, Tokyo, 113-8656, Japan
**Corresponding author: mori@ginjo.t.u-tokyo.ac.jp*

Abstract: We demonstrate unrepeated 200-km transmission of 40-Gbit/s 16-QAM signals using a digital coherent receiver, where the decision-directed carrier-phase estimation is employed. The phase fluctuation is effectively eliminated in the 16-QAM system with such a phase-estimation method, when the linewidth of semiconductor lasers for the transmitter and the local oscillator is 150 kHz. Finite-impulse-response (FIR) filters at the receiver compensate for 4,000-ps/nm group-velocity dispersion (GVD) of the 200-km-long single-mode fiber and a part of self-phase modulation (SPM) in the digital domain. In spite of the launched power limitation due to SPM, the acceptable bit-error rate performance is obtained owing to high sensitivity of the digital coherent receiver.

OCIS codes: (060.1660) Coherent communications; (060.4080) Modulation; (060.2920) Homodyning.

References and links

1. P. J. Winzer and R. -J. Essiambre, "Advanced optical modulation formats," Chapter 2 in *Optical Fiber Telecommunications* V B (edited by I. P. Kaminow, T. Li, and A.E. Willner, Academic Press, 2008).
2. L. E. Nelson, S. L. Woodward, M. D. Feuer, X. Zhou, P. D. Magill, S. Foo, D. Hanson, D. McGhan, H. Sun, M. Moyer, and M. O'Sullivan, "Performance of a 46-Gbps Dual-Polarization QPSK Transceiver in a High-PMD Fiber Transmission Experiment," in *Optical Fiber Communication Conference and Exposition and The National Fiber Optic Engineers Conference*, OSA Technical Digest (CD) (Optical Society of America, 2008), paper PDP9. http://www.opticsinfobase.org/abstract.cfm?URI=OFC-2008-PDP9.
3. X. Zhou, J. Yu, D. Qian, T. Wang, G. Zhang, and P. Magill "8x114 Gb/s, 25-GHz-spaced, polmux-RZ-8PSK transmission over 640 km of SSMF employing," Optical Fiber Communication Conference 2008, paper PDP6.
4. K. Kikuchi, "Phase-diversity homodyne detection of multilevel optical modulation with digital carrier phase estimation," IEEE J. Sel. Top. Quantum Electron. **12**, 563-570 (2006).
5. M. Yoshida, H. Goto, K. Kasai, and M. Nakazawa, "64 and 128 coherent QAM optical transmission over 150 km using frequency-stabilized laser and heterodyne PLL detection," Opt. Express **16**, 829-840 (2008).
6. M. Seimetz, " Performance of Coherent Optical Square-16-QAM-Systems Based on IQ-Transmitters and Homodyne Receivers with Digital Phase Estimation," in *Optical Fiber Communication Conference and Exposition and The National Fiber Optic Engineers Conference*, Technical Digest (CD) (Optical Society of America, 2006), paper NWA4. http://www.opticsinfobase.org/abstract.cfm?URI=NFOEC-2006-NWA4
7. M. Seimetz, "Laser Linewidth Limitations for Optical Systems with High-Order Modulation Employing Feed Forward Digital Carrier Phase Estimation," in *Optical Fiber Communication Conference and Exposition and The National Fiber Optic Engineers Conference*, OSA Technical Digest (CD) (Optical Society of America, 2008), paper OTuM2. http://www.opticsinfobase.org/abstract.cfm?URI=OFC-2008-OTuM2.
8. Y. Mori, C. Zhang, K. Igarashi, K. Katoh, and K. Kikuchi, "Unrepeated 200-km transmission of 40-Gbit/s 16-QAM signals using digital coherent optical receiver," Opto-Electronics and Communications Conference 2008, paper PDP-4.
9. Y. Mori, C. Zhang, K. Igarashi, K. Katoh, and K. Kikuchi, "Transmission of 40-Gbit/s 16-QAM Signal over 100-km Standard Single-mode Fiber using Digital Coherent Optical Receiver," European Conference on Optical Communication 2008, paper Tu.1.E.4.
10. S. Haykin, *Adaptive filter theory*, (Prentice Hall, 2001).

#104364 - $15.00 USD Received 20 Nov 2008; revised 15 Dec 2008; accepted 14 Jan 2009; published 23 Jan 2009

11. K. Kikuchi, T. Okoshi, M. Nagamatsu, and N. Henmi, "Degradation of bit-error rate in coherent optical communications due to spectral spread of transmitter and the local oscillator," J. Lightwave Technol. **2**, 1024-1033 (1984).
12. K. Kikuchi and S. Tsukamoto, "Evaluation of sensitivity of the digital coherent receiver," J. Lightwave Technol. **26**, 1817-1822 (2008).

1. Introduction

The use of multilevel modulation formats is one of the most effective ways of enhancing the spectral efficiency in optical fiber communication systems [1]. Among various modulation formats, *M*-ary phase-shift keying (PSK) such as quadrature PSK (QPSK) [2] and 8-PSK [3] has been extensively studied in conjunction with the digital coherent optical receiver, which enables restoration of the in-phase and quadrature components of the optical complex amplitude [4]. However, as far as the PSK format is employed, further increase in the level of modulation becomes difficult, because the distance between symbols on the complex plane is too short to maintain the bit-error rate (BER) performance.

On the other hand, quadrature amplitude modulation (QAM), where both of the in-phase and quadrature components are modulated in a multilevel manner [5], is the best candidate for the spectrally efficient modulation format, because we can minimize the power penalty due to the increase in the level of modulation.

However, in order to demodulate such QAM signals, we need to estimate the phase fluctuation, which stems from semiconductor lasers used for the transmitter and the local oscillator (LO). Although the carrier-phase estimation method which calculates 4-th power of the complex amplitude of the QAM signal was proposed [6, 7], rather complicated amplitude discrimination must be introduced before carrier-phase estimation. In contrast, we have proposed the much simpler decision-directed carrier-phase estimation, which is based on the least-mean square (LMS) algorithm. Transmission of 40-Gbit/s 16-QAM signals has been demonstrated by using this method [8, 9].

In this paper, we theoretically evaluate the phase-noise tolerance of the 10-Gsymbol/s 16-QAM system, where the decision-directed carrier-phase estimation is employed in the digital coherent receiver. Next, using such a digital coherent receiver, we demonstrate unrepeated 200-km transmission of the 40-Gbit/s 16-QAM signal. We can compensate for group-velocity dispersion (GVD) of 4,000 ps/nm and a part of self-phase modulation (SPM) by digital finite-impulse-response (FIR) filters after detection. The maximum launched power is limited to around 10 dBm by fiber nonlinearity; however, owing to the high back-to-back receiver sensitivity of -35 dBm at BER=10^{-5}, we can transmit the 16-QAM signal over an unrepeated distance of 200 km, where the link loss is 40 dBm.

2. Principle of decision-directed carrier-phase estimation

Figure 1 shows the block diagram of the decision-directed carrier-phase estimation, which is based on a one-tap FIR filter and the LMS algorithm to control its tap coefficient. $x(n)$ is the digitized complex amplitude detected by the homodyne phase-diversity receiver, where n denotes the number of sequence. $c(n)$ represents the tap coefficient which rotates $x(n)$ on the complex plane. The normalized LMS algorithm is given [10] by

$$c(n+1) = c(n) + \frac{\mu}{|x(n)|^2} e(n) x^*(n) \quad , \tag{1}$$

$$e(n) = d(n) - c(n)x(n) \quad , \tag{2}$$

where $d(n)$ is the decoded symbol; $e(n)$ represents the estimation error defined as the difference between the rotated complex amplitude and the decoded symbol; and μ is called the step size parameter. In accordance with Eqs. (1) and (2), $c(n)$ is updated in a symbol-by-symbol manner so that $e(n)$ approaches to zero.

#104364 - $15.00 USD Received 20 Nov 2008; revised 15 Dec 2008; accepted 14 Jan 2009; published 23 Jan 2009

When μ<<1, current updating of the tap coefficient is influenced by preceding symbols, which improves the signal-to-noise ratio (SNR) of the obtained phase reference. Roughly speaking, the inverse of μ represents the effective averaging-span length. On the other hand, we cannot cope with the fast phase change occurring in such a long effective averaging-span length. These facts mean that we need to optimize the μ-value, depending on the SNR of the received signal and the linewidth of the transmitter laser and the LO.

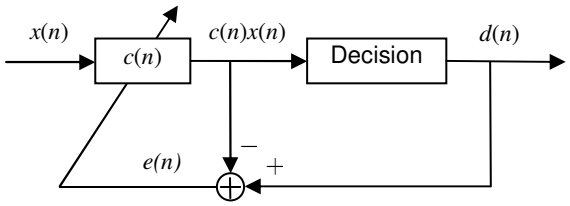

Fig. 1. Block diagram of the decision-directed carrier-phase estimation.

Figure 2 shows the computational framework of the decision-directed phase estimation. The part "c_k" includes the LMS-based calculation given by Eqs. (1) and (2). We find that this method is based on the feed-forward control scheme similar to the 4-th power method, and it is not difficult to implement a parallel-processing circuit. In contrast, the 4-th power phase estimation method for 16-QAM requires three-level amplitude discrimination before phase estimation, which increases computational complexity.

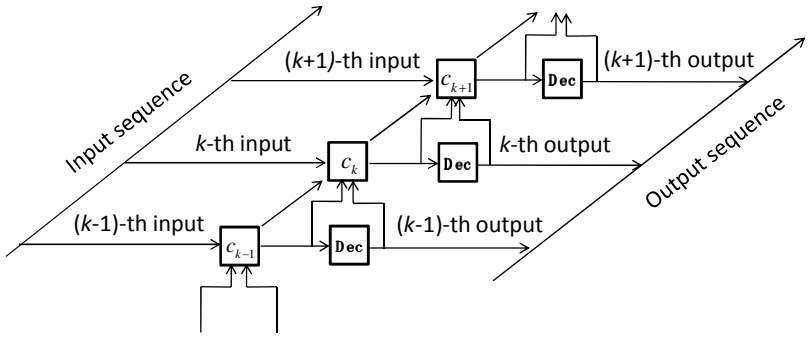

Fig. 2. Computational framework for decision-directed carrier-phase estimation. The part "c_k" includes the LMS-based calculation (Eqs.(1) and (2)). "Dec" represents the symbol decision circuit.

3. Simulation

In order to evaluate the phase-noise tolerance of the 16-QAM signal, we conducted computer simulations. The phase fluctuation of the restored complex amplitude has a Gaussian distribution given [11] by

$$\sigma^2 = 4\pi\delta f T \quad , \tag{3}$$

where δf represents the 3-dB spectral width of the transmitter as well as the local oscillator. T is the symbol duration, which is 100 ps in 10-Gsymbol/s systems. In this simulation, the intermediate frequency between the transmitter and the LO is assumed to be zero. The 16-QAM signal is differentially pre-coded.

#104364 - $15.00 USD Received 20 Nov 2008; revised 15 Dec 2008; accepted 14 Jan 2009; published 23 Jan 2009

Figure 3 shows BER characteristics calculated as a function of the SNR per bit. The linewidth of lasers for the transmitter and the LO is 0 Hz, 150 kHz, and 500 kHz in Figs. 2(a), (b), and (c), respectively, and the step size μ was used as a parameter ranging from 0.01 to 1.0. Figure 3(a) shows the case where the phase noise is negligible. We can find that as the step size decreases, the BER performance approaches the theoretical limit indicated by the broken curve. This is because the longer averaging-span length improves the SNR of the phase reference. However, when the laser linewidth is supposed to be 150 kHz, too small step size degrades the BER performance as shown in Fig. 3(b). This is due to the fact that the longer averaging-span length induces the larger phase error between the signal and the reference through the non-negligible laser phase noise. The value of the step size to obtain the best performance is 0.1, and the power penalty from the theoretical limit is about 1 dB at BER = 10^{-5} in such a case. As the laser linewidth is further increased to 500 kHz, the optimum value of the step size becomes 0.2, at which there remains the power penalty of 2 dB at BER=10^{-5}.

In this way, we can conclude that semiconductor lasers having a several-hundred-kHz linewidth are still applicable to 10-Gsymbol/s 16-QAM systems, provided that the phase-estimator circuit is properly designed. Although the optimized 4-th power method can also provide us with the almost similar BER performance, the decision-directed phase estimation scheme has a simpler configuration and an advantage that it can cope with any modulation format without structural modifications.

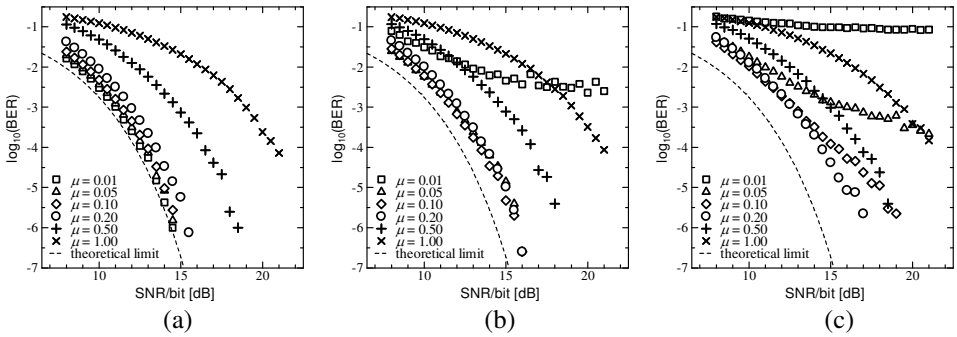

Fig. 3. Phase-noise tolerance of the 10-Gsymbol/s 16-QAM system, where the decision-directed carrier-phase estimation is employed. (a) δf = 0 Hz, (b) δf = 150 kHz, and (c) δf = 500 kHz.

4. Experimental setup

Figure 4 shows the experimental setup for measuring the transmission performance of the 16-QAM signal at 40 Gbit/s.

The laser for the transmitter was a distributed-feedback laser diode (DFB-LD). The wavelength of the DFB-LD was 1552 nm and its linewidth was about 150 kHz. Such a narrow linewidth was obtained by using DFB lasers with 1-mm device length. The beat frequency was kept less than 10 MHz through highly precise control of temperature and bias current. Simulation results show that the power penalty in such a case can be maintained below 1 dB. An NRZ 40-Gbit/s 16-QAM signal was produced by a $LiNbO_3$ optical IQ modulator (IQM). The IQM was driven by two streams of 4-level electrical signals generated from two independent ports of an arbitrary waveform generator (AWG). The electrical 16-QAM signal was differentially pre-coded, and each 4-level electrical signal formed a 2^9-1 pseudorandom pattern after decoding. The optical 16-QAM signal thus obtained was transmitted through a 200-km-long large-effective-core single-mode fiber (SMF). The effective core cross-section area was about 140 μm^2. The input power launched into the SMF was fixed at 10 dBm. After

#104364 - $15.00 USD Received 20 Nov 2008; revised 15 Dec 2008; accepted 14 Jan 2009; published 23 Jan 2009

200-km transmission, the accumulated GVD was 4,000 ps/nm and the total loss of the link was 40 dB.

In front of the receiver, the average power P_{in} was controlled by a variable optical attenuator (VOA). The receiver consisted of an erbium-doped fiber amplifier (EDFA) for pre-amplification and a homodyne phase-diversity receiver, where another DFB-LD having the same characteristics was used as a local oscillator. The reason why we employed the preamplifier is that only with a local oscillator, we could not achieve the shot-noise-limited receiver sensitivity by relatively large circuit noise. However, the sensitivity degradation due to such pre-amplification is as small as the spontaneous emission factor n_{sp} of the amplifier, which is half the noise figure and was 1 dB in our experiment.

The output from the receiver was asynchronously sampled at 20 Gsample/s by a two-channel analog-to-digital converter (ADC) with 8-bit resolution. The sampled data were then processed offline by the digital signal processing (DSP) circuit, which performed fixed FIR filtering for GVD compensation, clock recovery, decision-directed carrier-phase estimation, adaptive FIR filtering, and symbol decoding. The step size parameter μ of the carrier-phase estimator was set to 0.1, which was determined from simulation results in Sec.3. The adaptive FIR filter equalized the inter-symbol interference (ISI) due to imperfect IQ modulation and fiber nonlinearity to some extent. For ISI equalization, we applied the conventional LMS algorithm to update the complex tap coefficients of a 510-tap FIR filter.

LMS-based adaptive equalization can generally perform carrier phase recovery and ISI equalization at the same time. However, this statement is valid when the phase fluctuation of the signal is small enough. If we apply a single high-order FIR filter for such two purposes, the performances of the FIR filter is degraded as the filter delay increases. This is because the phase correlation between symbols with a long delay interval fades out due to large phase fluctuations occurring within the filter delay time. For this reason, we separated the function of FIR filtering into two parts: a one-tap FIR filter for carrier recovery in the first step and a multiple-tap FIR filter for ISI equalization in the second step.

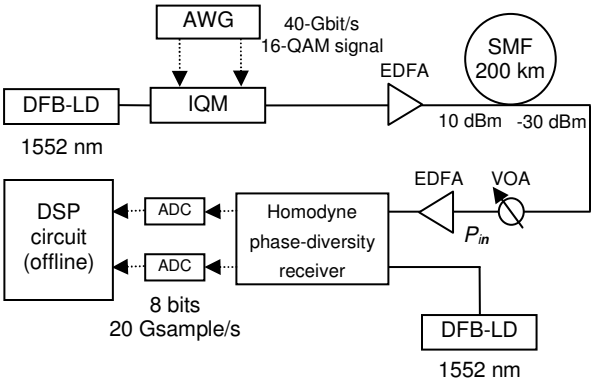

Fig. 4. Experimental setup for 16-QAM transmission.

5. Experimental results

Figure 5 illustrates constellation maps of 40-Gbit/s 16-QAM signals before (upper row) and after (lower row) adaptive equalization. Figures (a), (b) and (c) respectively show back-to-back constellation maps, and those after 100-km and 200-km transmission. The received average power is -30 dBm in every case.

From Fig. 5(a), we can find that the distortion of symbol alignment due to imperfect IQ modulation is improved drastically through adaptive equalization. After 100-km transmission

#104364 - $15.00 USD Received 20 Nov 2008; revised 15 Dec 2008; accepted 14 Jan 2009; published 23 Jan 2009

where the launched power was set to 0 dBm, although the fixed equalizer compensates for GVD, the effect of residual GVD has degraded the constellation map compared with the back-to-back one as shown in Fig. 5(b). From Fig. 5(c), we can observe that the distortion of symbol alignment begins to appear due to SPM at the launched power of 10 dBm: Note that the phase rotation angle is different among inner 4 symbols, middle 8 symbols, and outer 4 symbols. When we further increase the launched power, the distortion becomes more and more serious. Although symbols are realigned with adaptive filtering, SPM-induced ISI cannot be removed completely by the linear equalizing process, and the distribution of each equalized symbol is rather broad.

In Fig. 6, circles represent BERs of 40-Gbit/s 16-QAM signals after 200-km transmission, measured as a function of the received average power P_{in}. For comparison, back-to-back BERs and BERs after 100-km transmission are shown by crosses and squares, respectively, and the broken curve represents BERs in the shot-noise limit. Launching the average power of 10 dBm on the 200-km link, we can obtain the BER of $10^{-3.7}$, which is lower than the forward error correction (FEC) threshold. We find the 2-dB power penalty from the 100-km transmission result, which stems from SPM-induced ISI. In the case of 100-km transmission, we have the 5-dB penalty from the back-to-back result, which may be due to imperfect compensation for GVD by the fixed FIR filter. Residual GVD after the fixed FIR filter degrades the performance of the phase estimator because of the remaining waveform distortion. Such phase error degrades the bit-error performance, which cannot be recovered perfectly even by the adaptive equalizer.

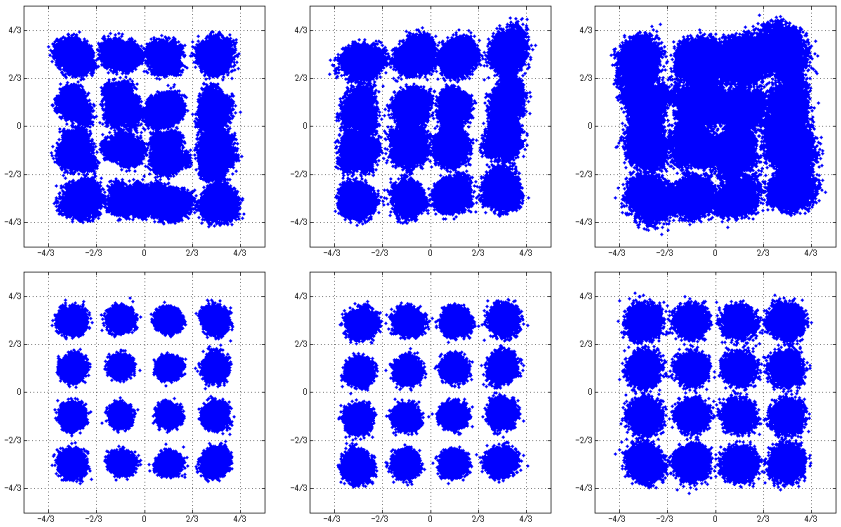

(a) (b) (c)

Fig. 5. Constellation maps of a 40-Gbit/s 16-QAM signal before (upper row) and after (lower row) adaptive equalization when P_{in} = -30 dBm. (a) back-to-back, (b) after 100-km transmission, and (c) after 200-km transmission.

#104364 - $15.00 USD Received 20 Nov 2008; revised 15 Dec 2008; accepted 14 Jan 2009; published 23 Jan 2009

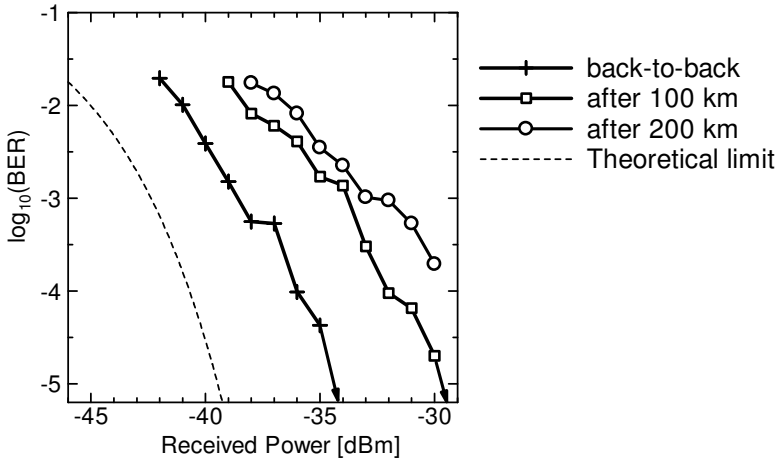

Fig. 6. BER characteristics of 40-Gbit/s 16-QAM signals measured as a function of the received average power P_{in}.

6. Conclusion

Based on computer simulations, we have evaluated the phase-noise tolerance of the 10-Gsymbol/s 16-QAM signal when the decision-directed carrier-phase estimation is employed. These results show that lasers having several-hundred-kHz linewidths are applicable to the 10-Gsymbol/s 16-QAM system. Next, we have demonstrated unrepeated 200-km transmission of the 40-Gbit/s 16-QAM signal using a digital coherent optical receiver. Although the digital FIR filter compensates for 4,000-ps/nm GVD, SPM-induced ISI degrades the BER performance; however, optimizing the launched power at around 10 dBm, we can obtain the acceptable BER better than the FEC threshold.

Acknowledgements

This work was supported in part by Strategic Information and Communications R&D Promotion Programme (SCOPE), Ministry of Internal Affairs and Communications, Japan.

#104364 - $15.00 USD Received 20 Nov 2008; revised 15 Dec 2008; accepted 14 Jan 2009; published 23 Jan 2009